

# Ferromagnetic resonance study of the free-hole contribution to magnetization and magnetic anisotropy in modulation-doped $\text{Ga}_{1-x}\text{Mn}_x\text{As}/\text{Ga}_{1-y}\text{Al}_y\text{As}:\text{Be}$

X. Liu, W. L. Lim, M. Dobrowolska, and J. K. Furdyna

*Department of Physics, University of Notre Dame, Notre Dame, Indiana 46556, USA*

T. Wojtowicz

*Department of Physics, University of Notre Dame, Notre Dame, Indiana 46556, USA*

*and Institute of Physics, Polish Academy of Sciences, 02-668, Warsaw, Poland*

(Received 14 July 2004; revised manuscript received 18 October 2004; published 7 January 2005)

Ferromagnetic resonance (FMR) is used to study magnetic anisotropy of GaMnAs in a series of  $\text{Ga}_{1-x}\text{Mn}_x\text{As}/\text{Ga}_{1-y}\text{Al}_y\text{As}$  heterostructures modulation-doped by Be. The FMR experiments provide a direct measure of cubic and uniaxial magnetic anisotropy fields and their dependence on the doping level. It is found that the increase in doping—in addition to raising the Curie temperature of the  $\text{Ga}_{1-x}\text{Mn}_x\text{As}$  layers—also leads to a very significant increase of their uniaxial anisotropy field. The FMR measurements further show that the effective  $g$ -factor of  $\text{Ga}_{1-x}\text{Mn}_x\text{As}$  is also strongly affected by the doping. This in turn provides a direct measure of the contribution from the free hole magnetization to the magnetization of the  $\text{Ga}_{1-x}\text{Mn}_x\text{As}$  system as a whole.

DOI: 10.1103/PhysRevB.71.035307

PACS number(s): 75.50.Pp, 76.30.-v, 76.50.+g, 75.70.Cn

## I. INTRODUCTION

Extensive studies of thin III-Mn-V films carried out during the past decade have confirmed the general model of hole-mediated ferromagnetism in these materials.<sup>1-6</sup> Although the details of the exchange interaction between the spins of Mn and of the valence-band holes—e.g., the sign of the exchange parameter  $N_0\beta$ —have not yet been unambiguously established, it is generally accepted that in the  $\text{III}_{1-x}\text{Mn}_x\text{V}$  systems the local Mn ions and the holes form one “global” complex bound together by strong magnetic exchange coupling. To understand magnetic phenomena in  $\text{III}_{1-x}\text{Mn}_x\text{V}$  materials—such as the interlayer exchange coupling,<sup>7</sup> formation of magnetic domains,<sup>8</sup> domain wall effects,<sup>9</sup> reorientation of the easy axis of magnetization,<sup>10</sup> etc.—it is therefore essential to investigate the properties of holes in these systems. For example, magnetic anisotropy<sup>11,12</sup>—which is expected to play a key role in future spin-based devices based on  $\text{III}_{1-x}\text{Mn}_x\text{V}$  alloys—is directly related to the anisotropy of the valence band characteristic of zinc blende III-V crystals.<sup>10,13-15</sup> Although many aspects of this relationship are now well understood, the correlation between magnetic anisotropy and hole concentration still holds many questions that are yet to be resolved.

It has recently been found that doping the  $\text{Ga}_{1-y}\text{Al}_y\text{As}$  barriers in  $\text{Ga}_{1-x}\text{Mn}_x\text{As}/\text{Ga}_{1-y}\text{Al}_y\text{As}$  heterostructures by Be acceptors leads to a significant increase of the Curie temperature  $T_C$  of the  $\text{Ga}_{1-x}\text{Mn}_x\text{As}$  layer.<sup>16</sup> These modulation-doped structures also provide a uniquely valuable tool for investigating hole-dependent physical properties, because one can vary the hole concentration  $n_h$  in these systems without disturbing the Mn concentration of the magnetic layer. This feature is extremely important, because in “normal”  $\text{III}_{1-x}\text{Mn}_x\text{V}$  layers there exists a strong correlation between the Fermi energy and Mn incorporation during the growth, so that changes in  $n_h$  automatically lead to changes in  $x$ , making

it difficult to separate the effect of the holes from those of Mn.<sup>17</sup>

It was also shown that ferromagnetic resonance (FMR) can be used for directly determining the magnetic anisotropy parameters of thin FM films.<sup>15,18,19</sup> In FMR the total magnetic moment of the Mn-ion/hole complex precesses *as a whole* around the direction of the total static magnetic fields present in the system (i.e., the applied magnetic field plus the magnetic anisotropy field) at the Larmor frequency  $\omega$ . In this work we use FMR to show that magnetic anisotropy in ultrathin modulation-doped GaMnAs films changes rapidly with the doping level for the same concentration of Mn. More importantly, FMR provides a unique way for determining the effective  $g$ -factor of the precessing Mn-ion/hole complex, and our results show that this “global”  $g$ -factor is strongly affected by the hole concentration. This last finding directly reflects the contribution of the free hole magnetization to the FMR dynamics of the GaMnAs system, and unambiguously confirms that the exchange interaction between the magnetic moments (not spins)<sup>20</sup> of Mn ions and of the holes is antiferromagnetic.

## II. SAMPLE FABRICATION AND EXPERIMENTAL PROCEDURE

Ferromagnetic  $\text{Ga}_{1-x}\text{Mn}_x\text{As}/\text{Ga}_{1-y}\text{Al}_y\text{As}$  heterostructures were grown on semi-insulating (001) GaAs substrates by molecular beam epitaxy (MBE), as described in detail in Ref. 16. Three heterostructures were used in the present study, all three consisting of a 5.6 nm  $\text{Ga}_{1-x}\text{Mn}_x\text{As}$  layer ( $x=0.06$ ) followed by a 13.5 nm  $\text{Ga}_{0.76}\text{Al}_{0.24}\text{As}$  barrier doped with Be starting at the distance of 1 monolayer away from the  $\text{Ga}_{1-x}\text{Mn}_x\text{As}$  layer. In preparing specimens with different doping levels the Be flux was kept constant during the growth, but the thickness of the doped region  $d_{\text{Be}}$  was varied,  $d_{\text{Be}}=0$  (undoped control sample No. 1), 5.3 nm (sample No.

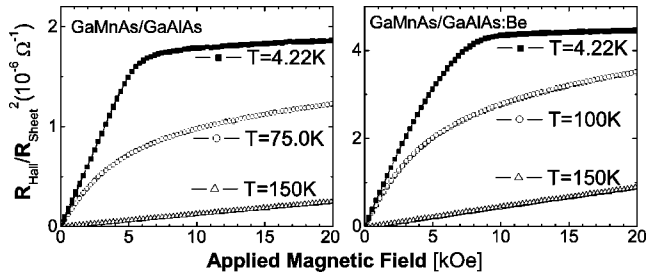


FIG. 1. Magnetization curves deduced from AHE at various temperatures for samples Nos. 1 and 3. Magnetic field  $\mathbf{H}$  is applied along the hard axis of magnetization,  $\mathbf{H} \parallel [001]$ .

2) and 13.2 nm (sample No. 3). A Quantum Design SQUID magnetometer was used for the magnetization measurement as a function of field and temperature. All three specimens showed similar values of remanent in-plane magnetization at low temperature (around  $30 \text{ emu/cm}^3$  at  $T=5 \text{ K}$ ).

The FMR measurements were carried out at 9.38 GHz using a Bruker electron paramagnetic resonance (EPR) spectrometer. The experimental setup and the polar coordinate system used in the subsequent discussion were described in detail in Ref. 15. Each heterostructure was cleaved into three  $2 \text{ mm} \times 2 \text{ mm}$  square pieces with edges along the  $[110]$  and  $[1\bar{1}0]$  directions, and the square pieces were mounted in the EPR bridge with either the  $[1\bar{1}0]$ , the  $[110]$ , or the  $[010]$  directions pointing vertically. With the dc magnetic field  $\mathbf{H}$  in the horizontal plane, this allowed us to map out the FMR for  $\mathbf{H}$  at any angle  $\theta_H$  between  $\mathbf{H} \parallel [001]$  (normal to the layer plane) and either of the three in-plane orientations,  $\mathbf{H} \parallel [110]$ ,  $[1\bar{1}0]$ , and  $[100]$ , following the same procedure as in Ref. 15.

### III. EXPERIMENTAL RESULTS

Because the GaMnAs layers under consideration are extremely thin ( $\sim 6 \text{ nm}$ ), direct magnetization measurements by SQUID were found to be insufficiently accurate. Instead, we made use of the fact that the anomalous Hall effect (AHE) is dominated by the magnetization  $M$ , and can thus serve as a measure of that parameter. To obtain the value of  $M$ , in our analysis we assumed that AHE is dominated by side-jump scattering—i.e., that  $M \propto R_{\text{Hall}}/R_{\text{sheet}}^2$ , where  $R_{\text{Hall}}$  is the Hall resistance and  $R_{\text{sheet}}$  is the sheet resistance when  $\mathbf{H}$  is applied perpendicular to the layer.<sup>17</sup> Typical magneto-transport data  $R_{\text{Hall}}/R_{\text{sheet}}^2$  are shown in Fig. 1 for several temperatures. Note that at  $T=4.22 \text{ K}$  the magnetization saturates at higher fields in modulation-doped samples (above 6.5 kOe; right-hand panel) than in undoped material (about 5.0 kOe; left-hand panel), thus indicating that the anisotropy field has been modified by the doping.

The inset in Fig. 2 shows FMR spectra at 4.0 K for a modulation-doped GaMnAs/GaAlAs:Be film (sample No. 3) in four basic configurations:  $\mathbf{H} \parallel [001]$ ,  $\mathbf{H} \parallel [110]$ ,  $\mathbf{H} \parallel [1\bar{1}0]$ , and  $\mathbf{H} \parallel [100]$ . Strikingly, sharp FMR peaks are observed in all configurations (and persist up to  $T_C$ ), indicating strong long-range FM coherence of the  $\text{Mn}^{++}$  spins. We find this remarkable, since the 5.6 nm thick  $\text{Ga}_{0.94}\text{Mn}_{0.06}\text{As}$  film is

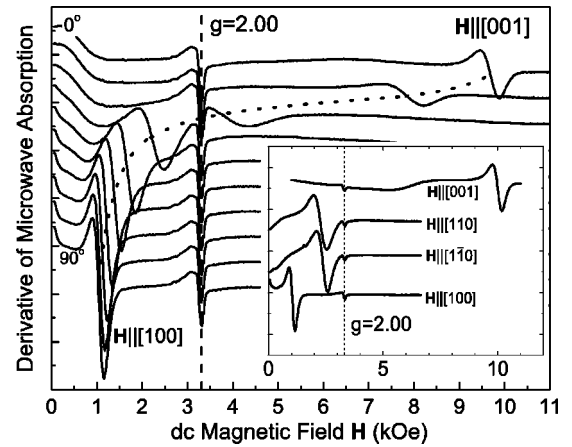


FIG. 2. FMR spectra observed at  $T=4 \text{ K}$  for sample No. 3 at various orientations  $\theta_H$  (from  $0^\circ$  to  $90^\circ$  in  $10^\circ$  increments) for  $\mathbf{H}$  between  $[100]$  and  $[001]$  directions in the  $(010)$  plane. The dotted line is a guide for the eye, indicating the shifting FMR position. The inset shows FMR spectra for the perpendicular ( $\mathbf{H} \parallel [001]$ ) and three parallel ( $\mathbf{H} \parallel [110]$ ,  $\mathbf{H} \parallel [1\bar{1}0]$ , and  $\mathbf{H} \parallel [100]$ ) configurations observed at 4.0 K. The weak peaks observed at the  $g=2.00$  resonance position (indicated by the vertical dashed line) are ascribed to EPR of isolated paramagnetic  $\text{Mn}^{++}$  ions.

approximately equivalent to only one monolayer of Mn ions randomly distributed over the specimen. As shown in Fig. 2, for intermediate orientations of  $\mathbf{H}$  between  $\mathbf{H} \parallel [100]$  and  $\mathbf{H} \parallel [001]$  the FMR peak  $H_R$  shifts from 1 kOe to 10 kOe. By their strong dependence on crystal geometry, the FMR spectra in Fig. 2 thus establish that magnetic anisotropy plays a major role in determining the fields at which the resonances occur.<sup>21</sup> We note parenthetically that a weak EPR peak is also observed around 3.3 kOe for all field orientations. This probably originates from a small fraction of isolated paramagnetic  $\text{Mn}^{++}$  ions with  $g=2.00$  either in the magnetic layer itself, or from  $\text{Mn}^{++}$  ions which have diffused into the AlGaAs barrier or the GaAs buffer.

The observation of sharp FMR spectra in these very thin specimens suggests that the magnetization is nearly homogeneous throughout each GaMnAs layer, and can thus be treated as a single magnetic moment precessing coherently around a dc magnetic field. One can therefore use the well-known Landau-Lifshitz-Gilbert (LLG) equation<sup>18,22</sup> to describe the FMR in these specimens. Following standard procedure, the magnetic anisotropy parameters of the magnetic films can then be obtained by analyzing the angular dependence of  $H_R$  using the following equations and the coordinate system defined in Ref. 15. For  $\varphi_H=45^\circ$  [ $\mathbf{H}$  and  $\mathbf{M}$  in the  $(1\bar{1}0)$  plane], the LLG equations give

$$\begin{aligned}
 (\omega/\gamma)^2 = & [H_R \cos(\theta_H - \theta) + (-4\pi M + H_{2\perp} + H_{4\perp}/2 \\
 & - H_{4\parallel}/4) \cos 2\theta + (H_{4\perp}/2 + H_{4\parallel}/4) \cos 4\theta] \\
 & \times [H_R \cos(\theta_H - \theta) + (-4\pi M + H_{2\perp} + H_{4\parallel}/2) \cos^2 \theta \\
 & + (H_{4\perp} + H_{4\parallel}/2) \cos^4 \theta - H_{4\parallel}]; \quad (1a)
 \end{aligned}$$

and for  $\varphi_H=0^\circ$  [ $\mathbf{H}$  and  $\mathbf{M}$  in the plane  $(010)$ ],

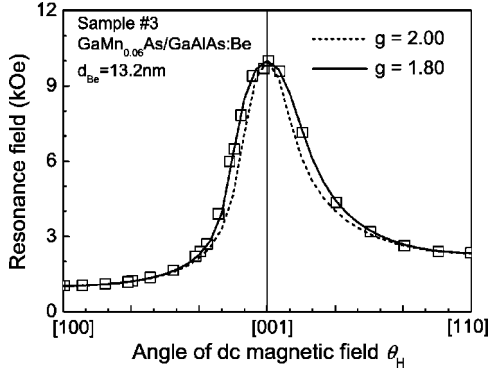


FIG. 3. Angular dependence of FMR positions for sample No. 3 for  $\mathbf{H}$  in the  $(1\bar{1}0)$  plane (right-hand panel), and for  $\mathbf{H}$  in the  $(010)$  plane (left-hand panel).

$$\begin{aligned}
 (\omega/\gamma)^2 = & [H_R \cos(\theta_H - \theta) + (-4\pi M + H_{2\perp} + H_{4\perp}/2 \\
 & - H_{4\parallel}/2)\cos 2\theta + (H_{4\perp}/2 + H_{4\parallel}/2)\cos 4\theta] \\
 & \times [H_R \cos(\theta_H - \theta) + (-4\pi M + H_{2\perp} - 2H_{4\parallel})\cos^2 \theta \\
 & + (H_{4\perp} + H_{4\parallel})\cos^4 \theta + H_{4\parallel}]. \quad (1b)
 \end{aligned}$$

Here  $H_{2\perp}$  and  $H_{4\perp}$  represent, respectively, the uniaxial and the cubic anisotropy fields perpendicular to the film; the anisotropy in the film plane is given by the cubic field  $H_{4\parallel}$ ;  $\omega$  is the angular microwave frequency; and  $\gamma = g\mu_B/\hbar$  is the gyromagnetic ratio,  $g$  being the spectroscopic splitting factor, and  $\hbar$  the Planck constant. To simplify the analysis, we have ignored the small in-plane uniaxial anisotropy field  $H_{2\parallel}$  associated with the difference between the  $[1\bar{1}0]$  and  $[110]$  axes.<sup>23</sup>

To determine the parameters appearing in Eq. (1), we first analyze the highly precise values of FMR fields  $H_R$  for the three high-symmetry directions ( $\mathbf{H}$  parallel to  $[100]$ ,  $[110]$ , and  $[001]$ ), following the procedure described in Ref. 15.<sup>24</sup> An independent determination of the  $g$ -factor and the three anisotropy fields  $H_{2\perp}$ ,  $H_{4\parallel}$ , and  $H_{4\perp}$  could not be achieved by the analysis of these values of  $H_R$  alone without additional information, since there are four variables but only three equations (those corresponding to  $\mathbf{H}$  parallel to  $[100]$ ,  $[110]$ ,

and  $[001]$ ). To reduce the number of variables (i.e., fitting parameters), we have first imposed the value of  $g=2.00$  of the individual  $\text{Mn}^{++}$  ions, as used in Ref. 15. With this constraint, the data for sample No. 3 at 4 K yield unique solutions of  $H_{2\perp} = -4319$  Oe,  $H_{4\parallel} = 739$  Oe, and  $H_{4\perp} = -1933$  Oe. Using these values in Eq. (1), we then obtain the angular variation of  $H_R$  shown by the dashed line in Fig. 3. The dashed curves clearly depart from the data, indicating that the assumption of  $g=2.00$ , while close, is not valid. On the other hand, we note that—due to the large in-plane compression of the GaMnAs film—the effect of the cubic  $H_{4\perp}$  term is expected to be completely overshadowed by  $H_{2\perp}$ , and may be neglected. In our second approach we have therefore assumed that  $H_{4\perp} = 0$ , treating  $g$ ,  $H_{4\parallel}$  and  $H_{2\perp}$  as fitting variables. With this approach, the data for sample No. 3 yield  $g = 1.80$ ,  $H_{4\parallel} = 720$  Oe, and  $H_{2\perp} = -5887$  Oe. Using these values (and  $H_{4\perp} = 0$ ) in Eq. (1), an excellent fit to the angular variation of  $H_R$  is obtained, as shown by the solid curve in Fig. 3.

It should be mentioned that one can obtain the effective anisotropy parameters and the  $g$ -factor in a self-consistent way by applying a recursive iterative fitting procedure to the angular-dependent FMR results, if one can determine  $H_{4\parallel}$  with sufficient accuracy.<sup>18</sup> We have therefore used the above results (based on assuming  $H_{4\perp} = 0$ ) as starting parameters to carry out a weighted nonlinear least squares fit to FMR positions for all values of  $\theta_H$  in both the  $(1\bar{1}0)$  and the  $(010)$  plane, allowing all four parameters ( $g$ ,  $H_{4\parallel}$ ,  $H_{2\perp}$ , and  $H_{4\perp}$ ) to vary. It is important to note that the difference between the two planes  $[(1\bar{1}0)$  and  $(010)]$  enables us to determine  $H_{4\parallel}$  very accurately, thus fulfilling the requirement just mentioned. The results obtained for all three specimens are listed in Table I. For example, the final iterative results for sample No. 3 are  $g = 1.80 \pm 0.02$ ,  $H_{2\perp} = -5764 \pm 90$  Oe,  $H_{4\parallel} = 735 \pm 20$  Oe, and  $H_{4\perp} = 8 \pm 110$  Oe. Note that the relation between the three anisotropy fields  $|H_{4\perp}| \ll |H_{4\parallel}| \ll |H_{2\perp}|$ , illustrated here (but holding for all samples) confirms our assumption that  $H_{4\perp}$  can be neglected as a first approximation. (Indeed,  $H_{4\perp}$  turns out to be much smaller than the fitting error.) Comparing these rigorous results with the parameters obtained from  $H_R$  observed for the three high-symmetry ori-

TABLE I. Key parameters for the  $\text{Ga}_{1-x}\text{Mn}_x\text{As}/\text{Ga}_{1-y}\text{Al}_y\text{As}$  heterostructures modulation-doped by Be. The anisotropy parameters and  $g$ -factors at 4 K are obtained by fitting the angular dependence of the FMR fields using Eq. (1). The values inside parentheses are obtained using the procedure in Ref. 15, i.e., using FMR fields for high-symmetry orientations and imposing the assumption that  $H_{4\perp} = 0$ .

Sample No.	1	2	3
Structure	GaMnAs/GaAlAs	GaMnAs/GaAlAs:Be	
$d_{\text{Be}}$ (nm)	0	5.3	13.2
$T_C$ (K)	72	85	95
$n_h$ -MF ( $\text{cm}^{-3}$ )	$1.24 \times 10^{20}$	$1.48 \times 10^{20}$	$1.64 \times 10^{20}$
$n_s$ -Hall ( $\text{cm}^{-2}$ )	$1.32 \times 10^{14}$	$1.74 \times 10^{14}$	$2.94 \times 10^{14}$
$H_{2\perp}$ (Oe)	$-3446 \pm 123$ ( $-3416$ )	$-5644 \pm 88$ ( $-5635$ )	$-5764 \pm 90$ (5887)
$H_{4\parallel}$ (Oe)	$1271 \pm 32$ (1260)	$738 \pm 20$ (727)	$735 \pm 20$ (720)
$H_{4\perp}$ (Oe)	$64 \pm 135$ (0)	$55 \pm 94$ (0)	$8 \pm 110$ (0)
$g_{\text{eff}}$	$1.92 \pm 0.04$ (1.92)	$1.87 \pm 0.03$ (1.87)	$1.80 \pm 0.02$ (1.80)

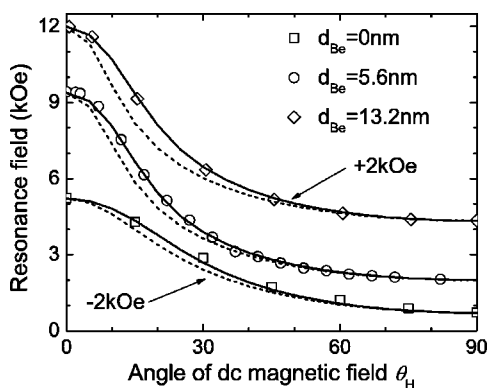


FIG. 4. Angular dependence of FMR positions at 4.0 K for  $\mathbf{H}$  in the  $(1\bar{1}0)$  plane for the three samples used in this study. Dashed curves show theoretical fits obtained for  $g=2.00$ ,  $H_{4\perp} \neq 0$ . The solid curves are fits obtained for  $H_{4\perp}=0$  and (top to bottom)  $g=1.80$ , 1.87, and 1.92.

entations ( $\mathbf{H}$  parallel to  $[100]$ ,  $[110]$ , and  $[001]$ ) under the assumption that  $H_{4\perp}=0$  for all three specimens shows that the two approaches lead to very similar values, as listed in Table I. In our analysis of the data observed as a function of temperature we will therefore use the simpler approach. Finally, we note that some anisotropy of the  $g$ -factor is expected in 2D quantum structures.<sup>25,26</sup> However, a fit obtained by replacing  $g$  with  $g=(g_{\parallel}^2 \sin^2 \theta + g_{\perp}^2 \cos^2 \theta)^{1/2}$  cannot be distinguished from the fit with an isotropic  $g$ -factor. We have therefore accepted an isotropic  $g$ -factor as an adequate approximation.

The  $g$ -factors and related magnetic properties for  $T=4$  K are listed in Table I for all three specimens under investigation. Although the sheet carrier densities  $n_s$ -Hall obtained from Hall measurements are not rigorously valid due to the AHE contribution, they nevertheless provide a useful indication of the *relative* level of the doping.<sup>27</sup> The values of the hole concentrations obtained from  $T_C$  using the mean field model,<sup>16</sup>  $n_h$ -MF, are also listed in Table I for comparison.

As listed in Table I and shown in Fig. 4, it is clear that the contribution of the holes to the  $g$ -factor is enhanced as hole concentration increases (i.e., the fits depart further from the  $g=2.00$  curves as the doping level increases). One should note here that modulation-doped samples used in this study provide an ideal tool for tracking the effect of holes on magnetic parameters of III-Mn-V alloys. This arises from the fact that the concentration of Mn (both substitutional and interstitial) is the same in all samples, because the deposition of the modulation-doped GaAlAs:Be layer *after* the GaMnAs layer has been grown does not affect the composition of the GaMnAs layer that is already in place.<sup>16,17</sup> The observed changes listed in Table I for all three samples—decrease of the  $g$ -factor with doping, enhancement of the uniaxial anisotropy field  $H_{2\perp}$ , and reduction of  $H_{4\parallel}$ —can thus only be ascribed to changes in the hole concentration.

#### IV. DISCUSSION

It is well known that in  $\text{Ga}_{1-x}\text{Mn}_x\text{As}$  grown by MBE different types of Mn-centers can be present. First, there are Mn

interstitials  $\text{Mn}_i$ ,<sup>28,29</sup> which in our specimens are estimated to constitute about 11% of the total Mn concentration.<sup>17</sup> The  $g$ -factor of  $\text{Mn}_i$  is unknown. However, it has been shown that  $\text{Mn}_i$  are attracted by Mn on the Ga sites ( $\text{Mn}_{\text{Ga}}$ ), tending to form antiferromagnetic  $\text{Mn}_i$ — $\text{Mn}_{\text{Ga}}$  pairs that are magnetically inactive.<sup>30</sup> And even without such pairing, it has been shown that the  $d$ -shells of  $\text{Mn}_i$  do not hybridize with the  $p$ -electrons of the valence band, and thus do not participate in the collective magnetization of the system.<sup>30</sup> Second, there exists the possibility of Mn antisites,  $\text{Mn}_{\text{As}}$ . The  $g$ -factor of  $\text{Mn}_{\text{As}}$  is also unknown. However, at As rich growth conditions it is very unlikely that a significant concentration of  $\text{Mn}_{\text{As}}$  is being created. Third, there are random Mn clusters, which account for less than 10% of the total Mn concentration in our specimens.<sup>17</sup> Most of these clusters are likely to occur in the form of MnAs precipitates, with a  $g$ -factor of Mn expected to be 2.0.<sup>31</sup> Finally, there are  $\text{Mn}^{++}$  ions substitutional at the Ga site,  $\text{Mn}_{\text{Ga}}$ . This latter case is more complicated, since  $\text{Mn}_{\text{Ga}}$  can occur either as ionized (or compensated) acceptors ( $A^-$ ), with  $g=2.0$ ; or as neutral acceptors ( $A^0$ ), with  $g=2.77$ .<sup>32,33</sup> Here one should note that the  $A^0$  centers have only been observed in highly insulating bulk GaAs:Mn crystals with extremely dilute Mn concentration (below  $10^{19} \text{ cm}^{-3}$ ), but never in  $\text{III}_{1-x}\text{Mn}_x\text{V}$  systems with Mn concentrations sufficient to exhibit ferromagnetism.<sup>34,35</sup> Since our  $\text{Ga}_{1-x}\text{Mn}_x\text{As}$  specimens are highly metallic and have Mn concentrations of about  $1.3 \times 10^{21} \text{ cm}^{-3}$  ( $x \approx 0.06$ ), we must assume that  $\text{Mn}_{\text{Ga}}$  occurs in the form of  $A^-$  acceptor centers, characterized by  $g=2.0$ .

For completeness, we note that in thin ferromagnetic films such as Ni-Fe films<sup>36</sup> one can observe  $g$ -factors that are thickness (or surface) dependent. These effects occur due to the lowering of crystal symmetry at interfaces in cases where the  $g$ -factor contains a significant orbital component. However, since the 5  $d$ -electrons of  $\text{Mn}^{++}$  constitute an exactly half-filled  $d$ -shell with a total orbital magnetic moment  $L^2=0$ ,<sup>37</sup> it is not expected that the surface or interface should affect the  $g$ -factor of  $\text{Mn}^{++}$  in zinc blende heterostructures.<sup>38</sup> Additionally, even if some interface effects were present, one must note that *all* our specimens have the same structural design, i.e., the same surfaces and interfaces, so that the effect on the  $g$ -factor from that source (if any) would not vary from sample to sample.

As a result of all arguments stated above, the effect of the hole concentration on the  $g$ -factors seen in Figs. 3 and 4 can be understood as follows. The total magnetization of GaMnAs has two components: a contribution from the  $\text{Mn}^{++}$  ions (more precisely, from the  $\text{Mn}_{\text{Ga}}^{++}$  ions that are not magnetically compensated by pairing with  $\text{Mn}_i$ ) arising from their pure-spin magnetic moments  $\mu_{\text{Mn}} = -g_{\text{Mn}} S_{\text{Mn}} \mu_B = 5.0 \mu_B$  (corresponding to  $g_{\text{Mn}}=2.00$  and  $S_{\text{Mn}}=-5/2$ ); and the contribution of free hole magnetic moments  $\mu_h$ , which include both spin and orbital components. We must thus consider the presence of two magnetically coupled sublattice magnetizations,  $M_{\text{Mn}} = n_{\text{Mn}} \mu_{\text{Mn}}$  and  $M_h = n_h \mu_h$ , where  $n_{\text{Mn}}$  and  $n_h$  are the effective concentrations of  $\text{Mn}_{\text{Ga}}^{++}$  and of the holes. To account for the coherent precession of such a coupled system, the  $g$ -factor present implicitly in Eq. (1) through the relation  $\gamma = g \mu_B \hbar^{-1}$  must be understood as an effective  $g$ -factor,  $g_{\text{eff}}$ , defined by<sup>39,40</sup>

$$\frac{n_{\text{Mn}}\mu_{\text{Mn}} + n_h\mu_h}{g_{\text{eff}}} = \frac{n_{\text{Mn}}\mu_{\text{Mn}}}{g_{\text{Mn}}} + \frac{n_h\mu_h}{g_h}, \quad (2)$$

where  $g_{\text{Mn}}$  and  $g_h$  are the  $g$ -factors corresponding to the  $\text{Mn}^{++}$  and hole sublattices.

We will first consider the result obtained for the undoped sample No. 1, for which we have obtained  $g_{\text{eff}}=1.92$ . Measurements on a “sister” sample (grown under identical conditions) have yielded  $n_{\text{Mn}}=(1.01\pm 0.10)\times 10^{21}\text{ cm}^{-3}$  and  $n_h=(1.24\pm 0.15)\times 10^{20}\text{ cm}^{-3}$ . With  $g_{\text{Mn}}=2.00$ ,  $\mu_{\text{Mn}}=5.00\mu_B$ , and  $g_{\text{eff}}=1.92$  we then have all the parameters in Eq. (2) for the undoped sample except  $g_h$  and  $\mu_h$ . To simplify the analysis, we treat the holes as pseudo-electrons, with an effective spin of  $S_h=\pm 1/2$  and a positive charge, so that  $\mu_h=g_h S_h \mu_B$ . The sign of  $S_h$  depends on the sign of the  $p$ - $d$  exchange integral  $N_0\beta$ . Despite its fundamental importance, the reader should note that various authors have reported widely different results for  $N_0\beta$  for the GaMnAs system, that vary in value and/or sign over the range from +2.5 eV (ferromagnetic exchange)<sup>41–43</sup> to -1.2 eV (antiferromagnetic exchange).<sup>13,44,45</sup> We will thus solve Eq. (2) for both  $S_h=+1/2$  and  $S_h=-1/2$ . If we take  $S_h=+1/2$ , we obtain  $g_h=-1.34$ , and thus  $\mu_h=-0.67\mu_B$ . For  $S_h=-1/2$  we obtain  $g_h=+5.18$ , which gives  $\mu_h=-2.6\mu_B$ . It is essential to note that—while the magnitudes of  $\mu_h$  for the two cases differ—both solutions indicate an antiferromagnetic alignment of the  $\text{Mn}^{++}$  and hole magnetic moments, pointing to the fact that the magnetization of the hole “sublattice” acts to reduce the overall magnetization of the Mn/hole collective system.

Having established the two possible values of  $g_h$  as discussed above, we can now solve Eq. (2) for the modulation doped cases.<sup>46</sup> Here the unknown parameter is  $n_h$ . As an illustration we consider the most highly doped sample No. 3, which yielded  $g_{\text{eff}}=1.80$ , again for the two possible signs of  $S_h$ . For  $S_h=+1/2$  (i.e.,  $g_h=-1.34$ ) and  $g_{\text{eff}}=1.80$ , Eq. (2) gives  $n_h=3.22\times 10^{20}\text{ cm}^{-3}$ , and for  $S_h=-1/2$  (i.e.,  $g_h=5.18$ ) we obtain  $n_h=2.99\times 10^{20}\text{ cm}^{-3}$ , with an error of about  $\pm 2\%$ . The similarity of the two values of  $n_h$  is most likely coincidental, but it is encouraging that both values have a reasonable order of magnitude.

Three interesting features emerge from the above analysis. First, regardless of the sign of  $S_h$  (i.e., the sign of  $N_0\beta$ ), the observation of  $g_{\text{eff}}<2.00$  results in a negative magnetic moment  $\mu_h$  of the holes (although without the *a priori* knowledge of the sign of  $S_h$  we cannot use our result to distinguish between  $\mu_h=-0.67\mu_B$  and  $\mu_h=-2.6\mu_B$ ). As a result, the magnetic moments (not spins)<sup>20</sup> of the Mn-ions and of the holes are *antiferromagnetically* coupled together, and the Mn-ion/hole complex can then be viewed as a *ferrimagnetic* system. Second, even with the uncertainty in the value of  $\mu_h$  we can use the results for  $n_h$  and  $\mu_h$  to estimate the ratio of the hole and the  $\text{Mn}^{++}$  contributions to the total magnetization  $M$ . For example, for the highly doped case of sample No. 3 ( $g_{\text{eff}}=1.80$ )  $M_h\approx -0.04M_{\text{Mn}}$  for  $S_h=+1/2$  and  $M_h\approx -0.15M_{\text{Mn}}$  for  $S_h=-1/2$ . And finally, in the modulation-doped case just analyzed the value of the hole concentration  $n_h=3.0\times 10^{20}\text{ cm}^{-3}$  is larger than the expected hole concentration estimated for that layer from its Curie temperature. It is possible that this discrepancy is caused by

our use of the value of  $g_h$  obtained for the undoped sample No. 1 in the analysis of the results obtained for the doped sample No. 3. Alternatively, this suggests the interesting possibility that some magnetic moment of the holes in the GaAlAs barrier may be coupled with the localized  $\text{Mn}^{++}$  spins in the GaMnAs layer by remote exchange coupling, and are thus expected to precess together with the magnetization of the GaMnAs layer as a single coherent system. We note in this connection that the Be doping of the barrier itself is estimated at approximately  $n_{\text{Be}}=3.0\times 10^{20}\text{ cm}^{-3}$ ,<sup>16</sup> which is in line with the above possibility. These results emphasize the need for an independent determination of the value of  $g_h$  for highly doped GaAs-based systems.

The fact that the holes of the  $\text{Ga}_{1-x}\text{Mn}_x\text{As}$  system contribute a finite magnetization has been predicted by many theoretical investigations.<sup>13,14,47</sup> For example, by considering the diamagnetic contribution from Landau currents associated with the spin-orbit interaction, Dietl *et al.* suggested that the magnetization of the free holes is opposite to the magnetization of the  $\text{Mn}^{++}$  sublattice in GaMnAs.<sup>13</sup> However, experimentally it is hard to separate out the hole contribution to the magnetization  $M$  using dc magnetization measurements, primarily due to the uncertainty of the effective Mn concentration (given the fact that Mn makes a much larger contribution to  $M$ ). However, the magnetization measurements definitely show that there is a magnetization deficit in GaMnAs system.<sup>48</sup> While there are several reasons which can cause this effect (removal of Mn from  $\text{Mn}_{\text{Ga}}$  to  $\text{Mn}_{\text{I}}$  sites;  $\text{Mn}_{\text{Ga}}\text{-Mn}_{\text{I}}$  pairing; and formation of Mn-based precipitates), the present results indicate that such deficit can also in part be attributed to the negative contribution of the holes to the total value of  $M$ . We should note therefore that in modulation-doped heterostructures we obtain significantly larger free hole concentrations compared to “normal” GaMnAs, making these systems especially well suited for studying the effect of holes on the overall magnetization of this alloy.

Measurements of FMR up to the Curie temperature  $T_C$  enable us to determine the temperature dependences of both the magnetic anisotropy fields and of the  $g$ -factor in modulation doped samples. These quantities, obtained using the four basic FMR geometries shown in the inset in Fig. 2 and assuming  $H_{4\perp}=0$ , are plotted in Fig. 5 for samples No. 1 (undoped; open symbols) and No. 3 (modulation doped; solid symbols). Results for sample No. 2 (not shown) lie in between the two sets of data seen in the figure. As shown in Fig. 5(a), FMR occurs above the  $g=2.00$  resonance position (horizontal dashed-dotted line) when  $\mathbf{H}$  is perpendicular to the film, and below that position for in-plane  $\mathbf{H}$  orientations. Shifts from the dashed-dotted line gradually decrease—and eventually vanish—as one approaches  $T_C$ . But clearly the modulation-doped sample has a much stronger shift (to our knowledge the strongest shift observed in any GaMnAs sample studied by FMR) than the undoped sample when  $\mathbf{H}$  is normal to the film, indicating a large increase of magnetic anisotropy due to the doping.

Figure 5(b) illustrates several basic features of magnetic anisotropy and its dependence on temperature and on the free hole concentration. First, we note that the cubic anisotropy fields decrease very rapidly with increasing  $T$ , while  $H_{2\perp}$

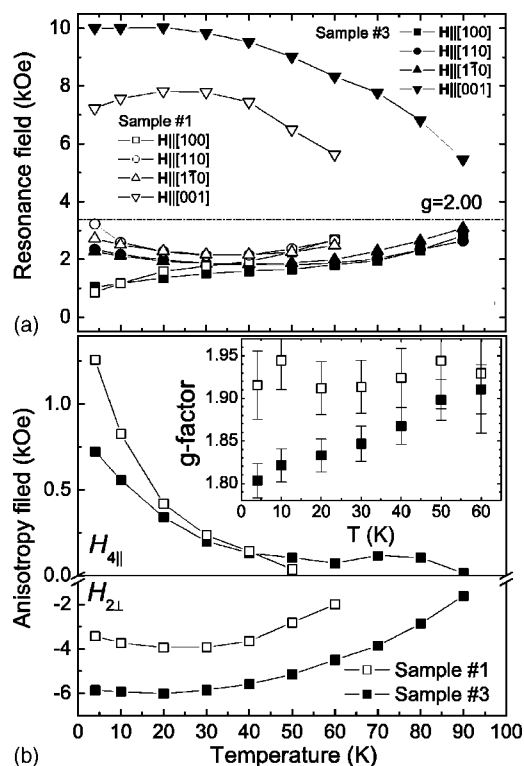


FIG. 5. Temperature dependence of the FMR results for undoped (sample No. 1, open symbols) and modulation-doped (sample No. 3, solid symbols) GaMnAs/GaAlAs heterostructures. (a) shows FMR positions observed for the four basic orientations of  $\mathbf{H}$  (same as in the inset in Fig. 2). Top and bottom panels of (b) show uniaxial and cubic anisotropy fields,  $H_{2\perp}$  and  $H_{4\parallel}$ , respectively, for the two samples. The effective  $g$ -factors for both samples are shown in the inset in (b).

drops off much more slowly. And second, modulation doping unambiguously increases the perpendicular uniaxial anisotropy field  $H_{2\perp}$ , while reducing the in-plane cubic field  $H_{4\parallel}$ . These observations are consistent with theoretical calculations predicting changes of magnetic anisotropy with hole concentration, although at this point the agreement is only qualitative. Finally, changes of the  $g$ -factor seen in the inset show a clear decreasing trend in doped samples below  $\sim 50$  K (in the inset we have restricted ourselves to data

obtained below ca. 50 K, since the error in determining  $g$ -values above that temperature is too large for a meaningful interpretation). While these  $g$ -factor values are only approximate, the clear low-temperature decrease of the  $g$ -factor seen in the doped sample may reflect the fact that the hole spins from the GaAlAs barrier increasingly couple with the magnetization in the GaMnAs layer as the temperature decreases, thus increasing the effect of Landau diamagnetism on the overall magnetization.

## V. CONCLUDING REMARKS

In conclusion, the results reported in this paper clearly point to the role which the valence-band holes play in determining both the magnetic anisotropy and the magnetization of  $\text{Ga}_{1-x}\text{Mn}_x\text{As}$ . Analysis of the angular dependence of FMR presented above shows unambiguously that the value of the effective  $g$ -factor of the Mn-ion/hole complex is lower than 2.00. This finding confirms that magnetization of the hole subsystem plays an essential role in the precession dynamics of the  $\text{Ga}_{1-x}\text{Mn}_x\text{As}$  magnetization as a whole. Specifically, the  $\text{Mn}^{2+}$  ion and hole sublattices are coupled antiferromagnetically to form a “global” Mn-ion/hole *ferrimagnetic* complex. In our most highly doped sample the magnitude of the magnetic contribution of the holes  $M_h$  was estimated to be of the order of 10% of the total magnetization  $M_{\text{total}}$ .

Our results have shown, further, that the coupling of the  $\text{Mn}^{2+}$  and of the hole magnetic moments is antiferromagnetic, no matter what sign of the  $p$ - $d$  exchange integral  $N_0\beta$  is taken. Thus the present results cannot be used as they stand to shed light on this parameter. If, however, one independently succeeds in determining the value of  $g_h$ , one could use the results presented here to establish the sign of  $N_0\beta$ . Since the knowledge of this exchange parameter is of key importance for our understanding of  $\text{III}_{1-x}\text{Mn}_x\text{V}$  alloys, it is our hope that results reported in this paper will stimulate interest in establishing the value of the hole  $g$ -factor (along with its dependence on the Fermi level) in highly doped GaAs-based alloys.

## ACKNOWLEDGMENTS

This work was supported by the DARPA SpinS Program and by NSF-NIRT Grant No. DMR02-10519.

<sup>1</sup>H. Ohno, *Science* **281**, 951 (1998).

<sup>2</sup>T. Dietl, H. Ohno, F. Matsukura, J. Cibert, and D. Ferrand, *Science* **287**, 1019 (2000).

<sup>3</sup>H. Ohno, *J. Magn. Magn. Mater.* **200**, 110 (1999).

<sup>4</sup>J. K. Furdyna, X. Liu, W. L. Lim, Y. Sasaki, T. Wojtowicz, I. Kuryliszyn, S. Lee, K. M. Yu, and W. Walukiewicz, *J. Korean Phys. Soc.* **42**, S579 (2003).

<sup>5</sup>J. König, J. Schliemann, T. Jungwirth, and A. H. MacDonald, in *Electronic Structure and Magnetism of Complex Materials*, edited by D. J. Singh and D. A. Papaconstantopoulos (Springer-Verlag, Berlin, 2003).

<sup>6</sup>S. T. B. Goennenwein, T. A. Wassner, H. Huebl, M. S. Brandt, J. B. Philipp, M. Opel, R. Gross, A. Koeder, W. Schoch, and A. Waag, *Phys. Rev. Lett.* **92**, 227202 (2004).

<sup>7</sup>S. J. Chung, S. Lee, I. W. Park, X. Liu, and J. K. Furdyna, *J. Appl. Phys.* **95**, 7402 (2004).

<sup>8</sup>U. Welp, V. K. Vlasko-Vlasov, X. Liu, J. K. Furdyna, and T. Wojtowicz, *Phys. Rev. Lett.* **90**, 167206 (2003).

<sup>9</sup>H. X. Tang, S. Masmanidis, R. K. Kawakami, D. D. Awschalom, and M. L. Roukes, *Nature (London)* **431**, 52 (2004).

<sup>10</sup>M. Sawicki, E. Matsukura, T. Dietl, G. M. Schott, C. Ruester, G. Schmidt, L. W. Molenkamp, and G. Karczewski, *J. Supercond.*

- 16**, 7 (2003).
- <sup>11</sup>G. P. Moore, J. Ferré, A. Mougin, M. Moreno, and L. Däweritz, *J. Appl. Phys.* **94**, 4530 (2003).
- <sup>12</sup>K. Hamaya, T. Taniyama, Y. Kitamoto, R. Moriya, and H. Munekata, *J. Appl. Phys.* **94**, 7657 (2003).
- <sup>13</sup>T. Dietl, H. Ohno, and F. Matsukura, *Phys. Rev. B* **63**, 195205 (2001).
- <sup>14</sup>M. Abolfath, T. Jungwirth, J. Brum, and A. H. MacDonald, *Phys. Rev. B* **63**, 054418 (2001).
- <sup>15</sup>X. Liu, Y. Sasaki, and J. K. Furdyna, *Phys. Rev. B* **67**, 205204 (2003).
- <sup>16</sup>T. Wojtowicz, W. L. Lim, X. Liu, M. Dobrowolska, J. K. Furdyna, K. M. Yu, W. Walukiewicz, I. Vurgaftman, and J. R. Meyer, *Appl. Phys. Lett.* **83**, 4220 (2003).
- <sup>17</sup>K. M. Yu, W. Walukiewicz, T. Wojtowicz, W. L. Lim, X. Liu, M. Dobrowolska, and J. K. Furdyna, *Appl. Phys. Lett.* **84**, 4325 (2004).
- <sup>18</sup>M. Farle, *Rep. Prog. Phys.* **61**, 755 (1998).
- <sup>19</sup>K. Dziatkowski, M. Palczewska, T. Słupiński, and A. Twardowski, *Phys. Rev. B* **70**, 115202 (2004).
- <sup>20</sup>This distinction needs to be made because the contribution of holes to the magnetization is determined by how their magnetic moments align themselves with the moments of the  $Mn^{++}$  ions; and magnetic moments of holes contain not only a spin, but also an orbital component.
- <sup>21</sup>Y. Sasaki, X. Liu, J. K. Furdyna, M. Palczewska, J. Szczytko, and A. Twardowski, *J. Appl. Phys.* **91**, 7484 (2002).
- <sup>22</sup>P. E. Wigen, *Phys. Rev.* **133**, A1557 (1964).
- <sup>23</sup>U. Welp, V. K. Vlasko-Vlasov, A. Menzel, H. D. You, X. Liu, J. K. Furdyna, and T. Wojtowicz, *Appl. Phys. Lett.* **85**, 260 (2004).
- <sup>24</sup>Note, however, that in Ref. 15 the in-plane magnetic uniaxial anisotropy was also included, while in the present samples this anisotropy is insignificantly small, and is therefore ignored.
- <sup>25</sup>P. Peyla, A. Wasiela, Y. Merle d'Aubigné, D. E. Ashenford, and B. Lunn, *Phys. Rev. B* **47**, 3783 (1993).
- <sup>26</sup>R. Winkler, S. J. Papadakis, E. P. De Poortere, and M. Shayegan, *Phys. Rev. Lett.* **85**, 4574 (2000).
- <sup>27</sup>D. Ruzmetov, J. Scherschligt, D. V. Baxter, T. Wojtowicz, X. Liu, Y. Sasaki, J. K. Furdyna, K. M. Yu, and W. Walukiewicz, *Phys. Rev. B* **69**, 155207 (2004).
- <sup>28</sup>K. M. Yu, W. Walukiewicz, T. Wojtowicz, I. Kuryliszyn, X. Liu, Y. Sasaki, and J. K. Furdyna, *Phys. Rev. B* **65**, 201303(R) (2002).
- <sup>29</sup>K. M. Yu, W. Walukiewicz, T. Wojtowicz, W. L. Lim, X. Liu, U. Bindley, M. Dobrowolska, and J. K. Furdyna, *Phys. Rev. B* **68**, 041308(R) (2003).
- <sup>30</sup>J. Blinowski and P. Kacman, *Phys. Rev. B* **67**, 121204(R) (2003).
- <sup>31</sup>T. Hartmann, M. Lampalzer, P. J. Klar, W. Stolz, W. Heimbrodt, H.-A. K. von Nidda, A. Loidl, and L. Svistov, *Physica E (Amsterdam)* **13**, 572 (2002).
- <sup>32</sup>J. Schneider, U. Kaufmann, W. Wilkening, M. Baeumler, and F. Köhl, *Phys. Rev. Lett.* **59**, 240 (1987).
- <sup>33</sup>O. M. Fedorych, E. M. Hankiewicz, Z. Wilamowski, and J. Sadowski, *Phys. Rev. B* **66**, 045201 (2002).
- <sup>34</sup>J. Szczytko, A. Twardowski, K. Swiatek, M. Palczewska, M. Tanaka, T. Hayashi, and K. Ando, *Phys. Rev. B* **60**, 8304 (1999).
- <sup>35</sup>J. Szczytko, A. Twardowski, M. Palczewska, R. Jabłoński, J. Furdyna, and H. Munekata, *Phys. Rev. B* **63**, 085315 (2001).
- <sup>36</sup>J. P. Nibarger, R. Lopusnik, Z. Celinski, and T. J. Silva, *Appl. Phys. Lett.* **83**, 93 (2003).
- <sup>37</sup>C. Kittel, *Introduction to Solid State Physics*, 7th ed. (Wiley, New York, 1995).
- <sup>38</sup>M. Qazzaz, G. Yang, S. H. Xin, L. Montes, H. Luo, and J. K. Furdyna, *Solid State Commun.* **96**, 405 (1995); J. K. Furdyna, M. Qazzaz, G. Yang, L. Montes, S. H. Xin, and H. Luo, *Acta Phys. Pol. A* **88**, 607 (1995).
- <sup>39</sup>B. Lax and K. J. Button, *Microwave Ferrites and Ferrimagnetics* (McGraw-Hill, New York, 1962); R. K. Wangsness, *Phys. Rev.* **91**, 1085 (1953).
- <sup>40</sup>M. Rubinstein, A. Hanbicki, P. Lubitz, M. Osofsky, J. J. Krebs, and B. Jonker, *J. Magn. Magn. Mater.* **250**, 164 (2002).
- <sup>41</sup>J. Szczytko, W. Mac, A. Stachow, A. Twardowski, P. Becla, and J. Tworzydło, *Solid State Commun.* **99**, 927 (1996).
- <sup>42</sup>A. Twardowski, *Mater. Sci. Eng., B* **63**, 96 (1999).
- <sup>43</sup>T. Hartmann, M. Lampalzer, W. Stolz, K. Megges, J. Lorberth, P. J. Klar, and W. Heimbrodt, *Thin Solid Films* **364**, 209 (2000).
- <sup>44</sup>J. Okabayashi, A. Kimura, O. Rader, T. Mizokawa, A. Fujimori, T. Hayashi, and M. Tanaka, *Phys. Rev. B* **58**, R4211 (1998).
- <sup>45</sup>J. Szczytko, W. Bardyszewski, and A. Twardowski, *Phys. Rev. B* **64**, 075306 (2001).
- <sup>46</sup>The value of  $g_h$  which enters Eq. (2)—while it is determined by the band structure—may also depend on the Fermi level. We are using the same value of this parameter because the difference in  $n_h$  is estimated to be only about 30%. We are aware, however, that this is an assumption that may lead to some error in the calculation of  $n_h$  for sample No. 3.
- <sup>47</sup>J. Schliemann, J. König, and A. H. MacDonald, *Phys. Rev. B* **64**, 165201 (2001).
- <sup>48</sup>S. J. Potashnik, K. C. Ku, R. Mahendiran, S. H. Chun, R. F. Wang, N. Samarth, and P. Schiffer, *Phys. Rev. B* **66**, 012408 (2002); S. J. Potashnik, K. C. Ku, R. F. Wang, M. B. Stone, N. Samarth, P. Schiffer, and S. H. Chun, *J. Appl. Phys.* **93**, 6784 (2003).